Climate
of the Past

Supplement of

Assessing transient changes in the ocean carbon cycle during the last deglaciation through carbon isotope modeling

Hidetaka Kobayashi et al.

Correspondence to: Hidetaka Kobayashi (hidekoba@sci.u-toyama.ac.jp)

Supplement

Contents of this file

Introduction

The supplementary information given here shows the biogeochemical changes obtained in numerical simulations, information on the core data used to compare with the simulation results, and figures comparing the data and simulation results needed to improve the comprehension of the discussion.

Streamfunction

(a) 21kaBP

(d) 13kaBP

(b) 17kaBP

(e) 12kaBP

(c) 15kaBP

(f) 11kaBP
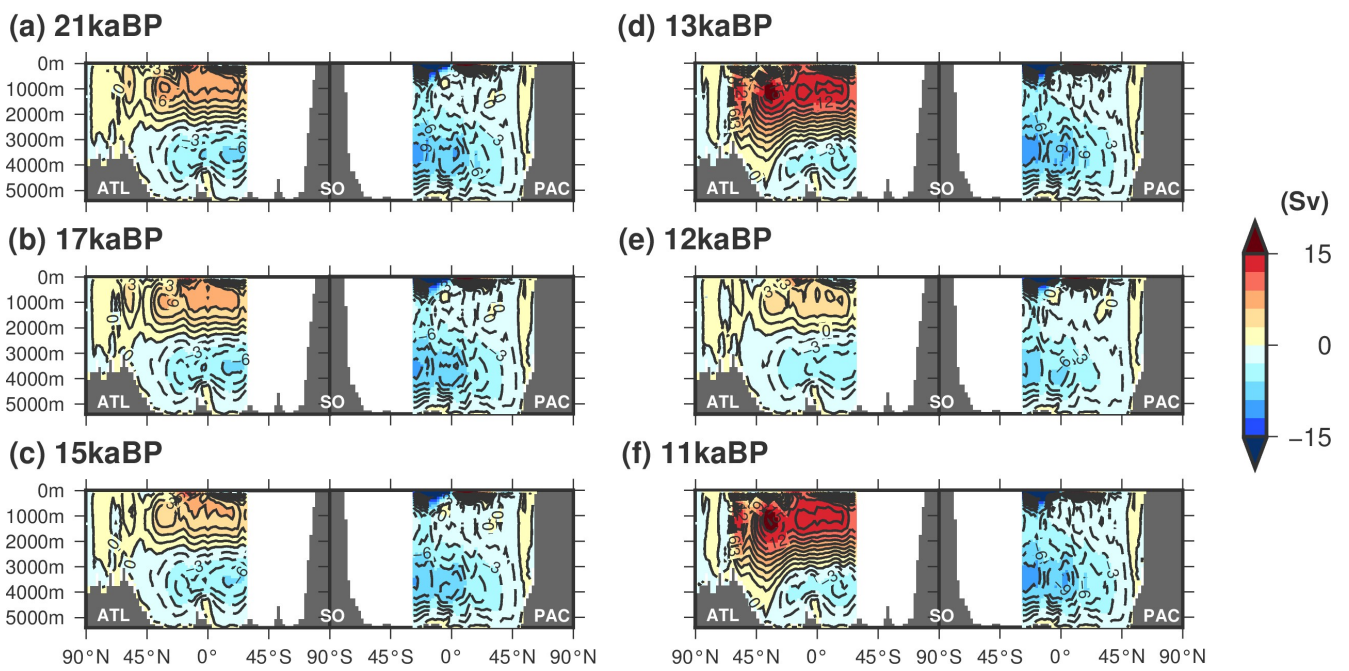
Figure S1: Ocean meridional streamfunctions (Sv : Sverdrup) are shown for the Atlantic (left) and Pacific (right). The contour interval is 1.5 Sv. The model output is averaged over a period of 100 years before and after each year of interest. The abbreviations for the oceans are ATL for Atlantic Ocean, SO for Southern Ocean, and PAC for Pacific Ocean.
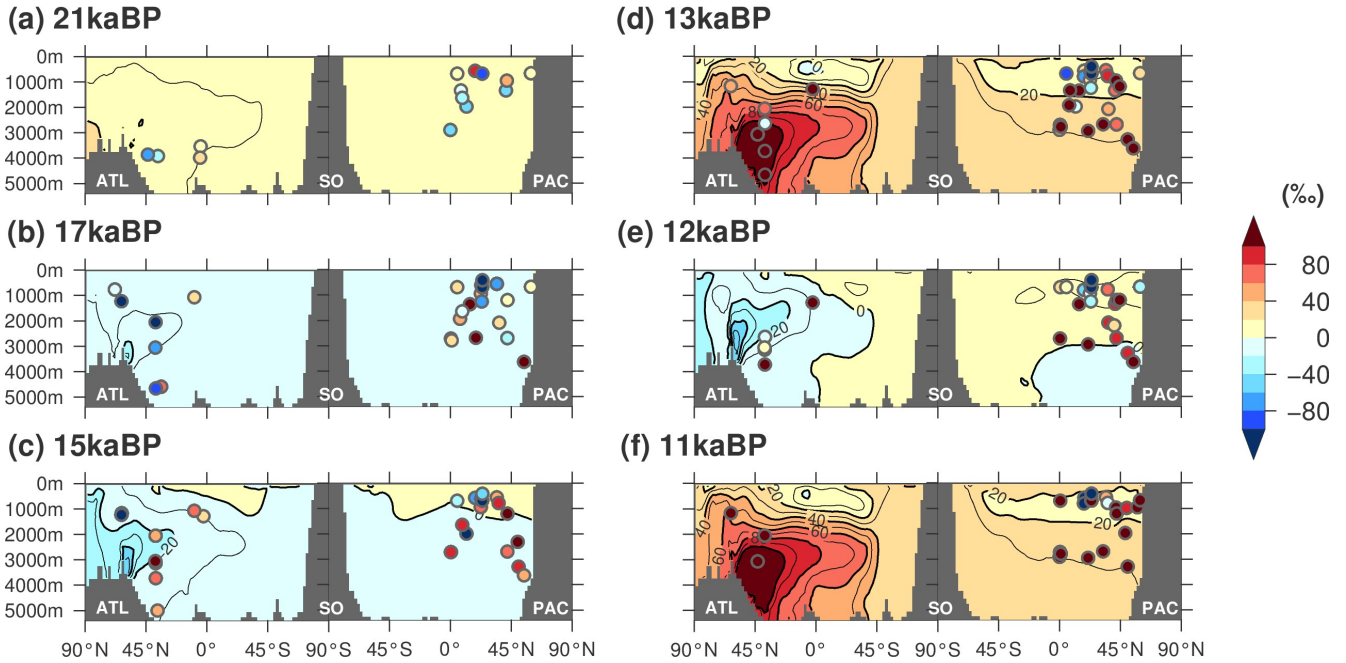
Figure S2: Oceanic zonal mean distribution of the difference in $\Delta\Delta^{14}C$ between the period of interest and the average of the 18–21 ka BP period in the Atlantic and Pacific oceans. The specific periods of interest include (a) the Last Glacial Maximum (21 ka BP), (b) Heinrich Stadial 1 (17 ka BP), (c) just before the Bølling–Allerød (BA) transition (15 ka BP), (d) the BA warm period (13 ka BP), (e) the Younger Dryas period (12 ka BP), and (f) the Holocene (11 ka BP). The contour interval is 10 ‰. The sediment core records used in the figure are compiled in *Rafter et al.,* (2022). Model results are averaged over 200 years, i.e., 100 years before and after each target year. However, for 21 ka BP, the average is taken from results spanning 21.0–20.9 ka BP; for 11 ka BP, the average is taken from results spanning 11.1–11.0 ka BP. The figure also includes a compilation of sediment core records where reconstructed values are plotted for 250 years before and after the target year. The vertical section represents all dat within the relevant ocean basins.
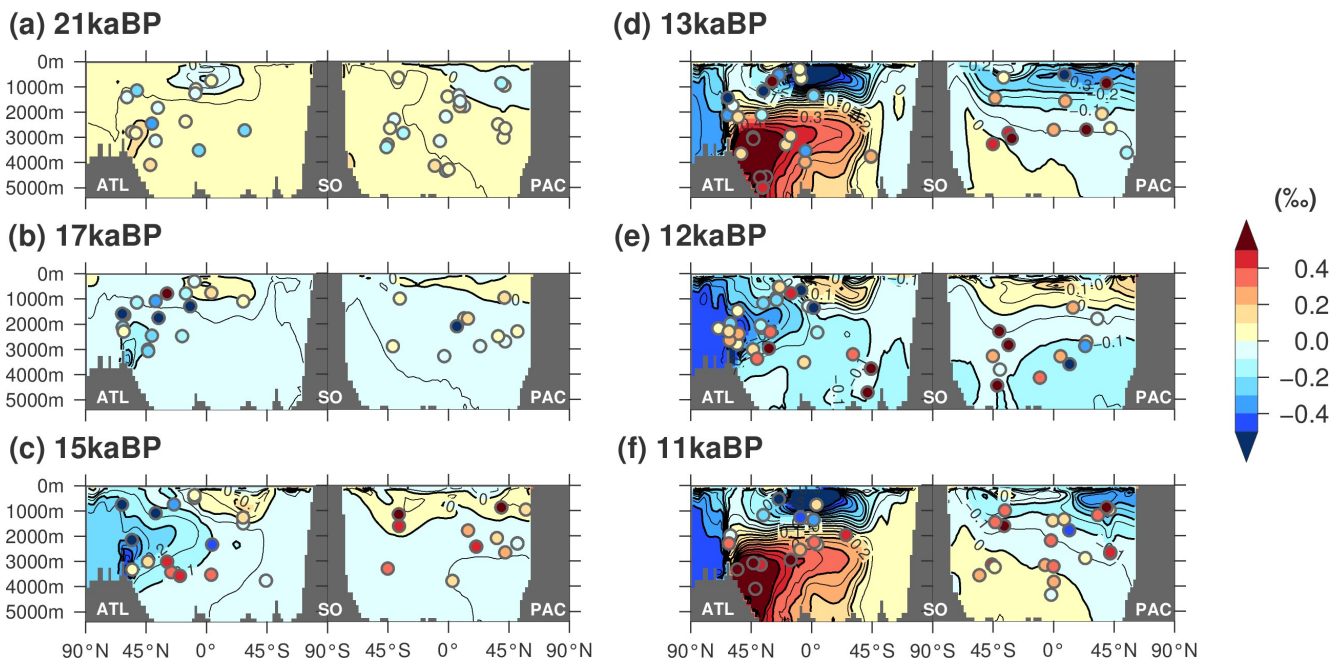
Figure S3: Oceanic zonal mean distribution of the difference in δ^{13}C between the period of interest and the average of the 18–21 ka BP period in the Atlantic and Pacific oceans. The contour interval is 0.05 ‰. The sediment core records used in the figure are compiled in *Muglia et al.*, (2023). The period over which the model output is averaged is 100 years before and after each year of interest. The reconstructed values are also plotted for 100 years before and after each year of interest.
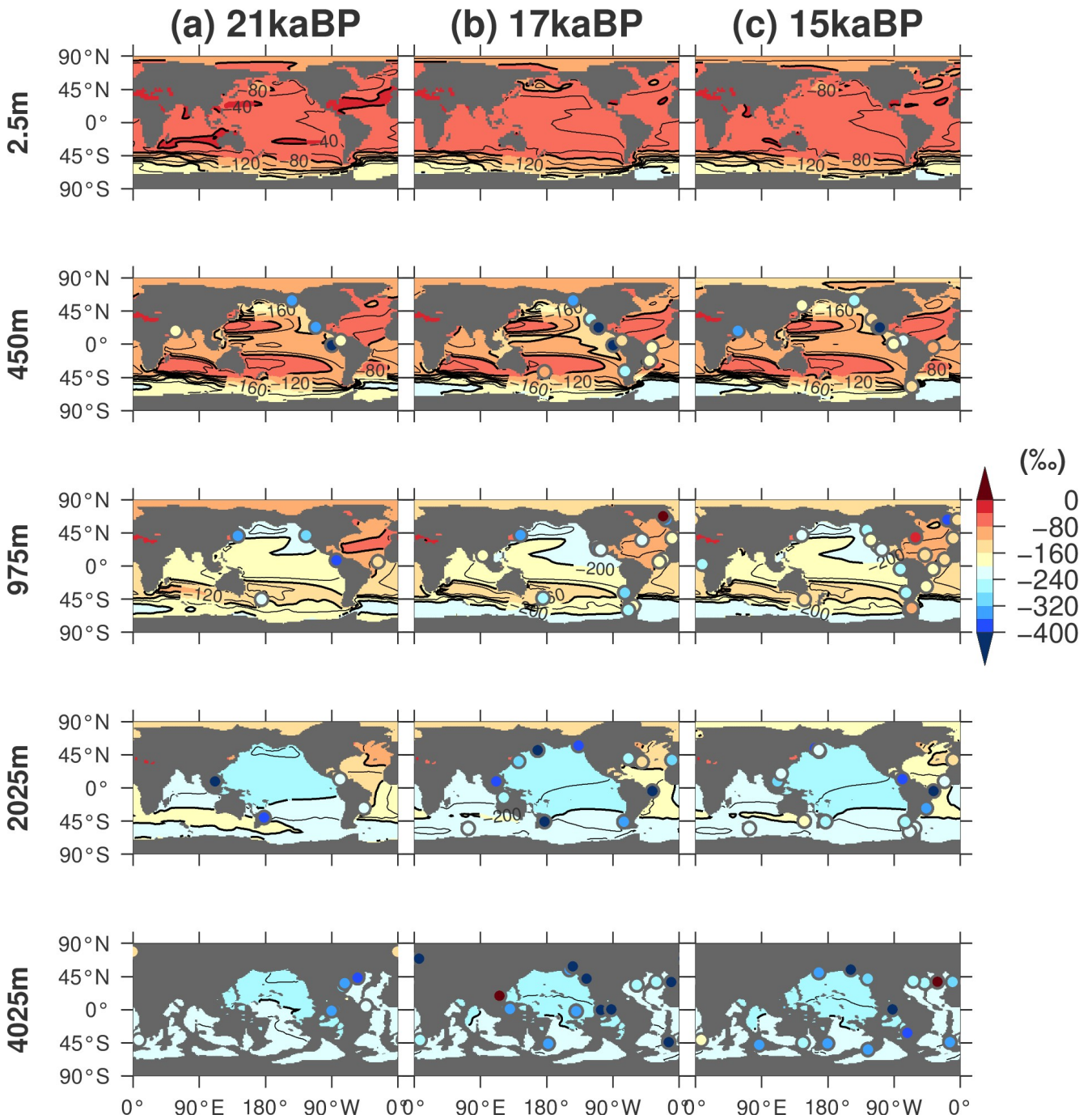
Figure S4: Oceanic distribution of $\Delta\Delta^{14}$C (‰) at specific depths (2.5 m, 450 m, 975 m, 2025 m, and 4025 m) during key periods of the last deglaciation. The specific periods of interest include the Last Glacial Maximum (21 ka BP), Heinrich Stadial 1 (17 ka BP), just before the Bølling-Allerød (BA) transition (15 ka BP), the BA warm period (13 ka BP), the Younger Dryas period (12 ka BP), and the Holocene (11 ka BP). The contour interval is 40 ‰. The sediment core records used in the figure are compiled in *Rafter et al.*, (2022). Model results are averaged over 200 years, i.e., 100 years before and after each target year. However, for 21 ka BP, the average is taken from results spanning 21.0–20.9 ka BP; for 11 ka BP, the average is taken from results spanning 11.1–11.0 ka BP. The figure also includes a compilation of sediment core records where reconstructed values are plotted for 250 years before and after the target year. The vertical section represents all dat within the relevant ocean basins.

5

Figure S4: (continued)
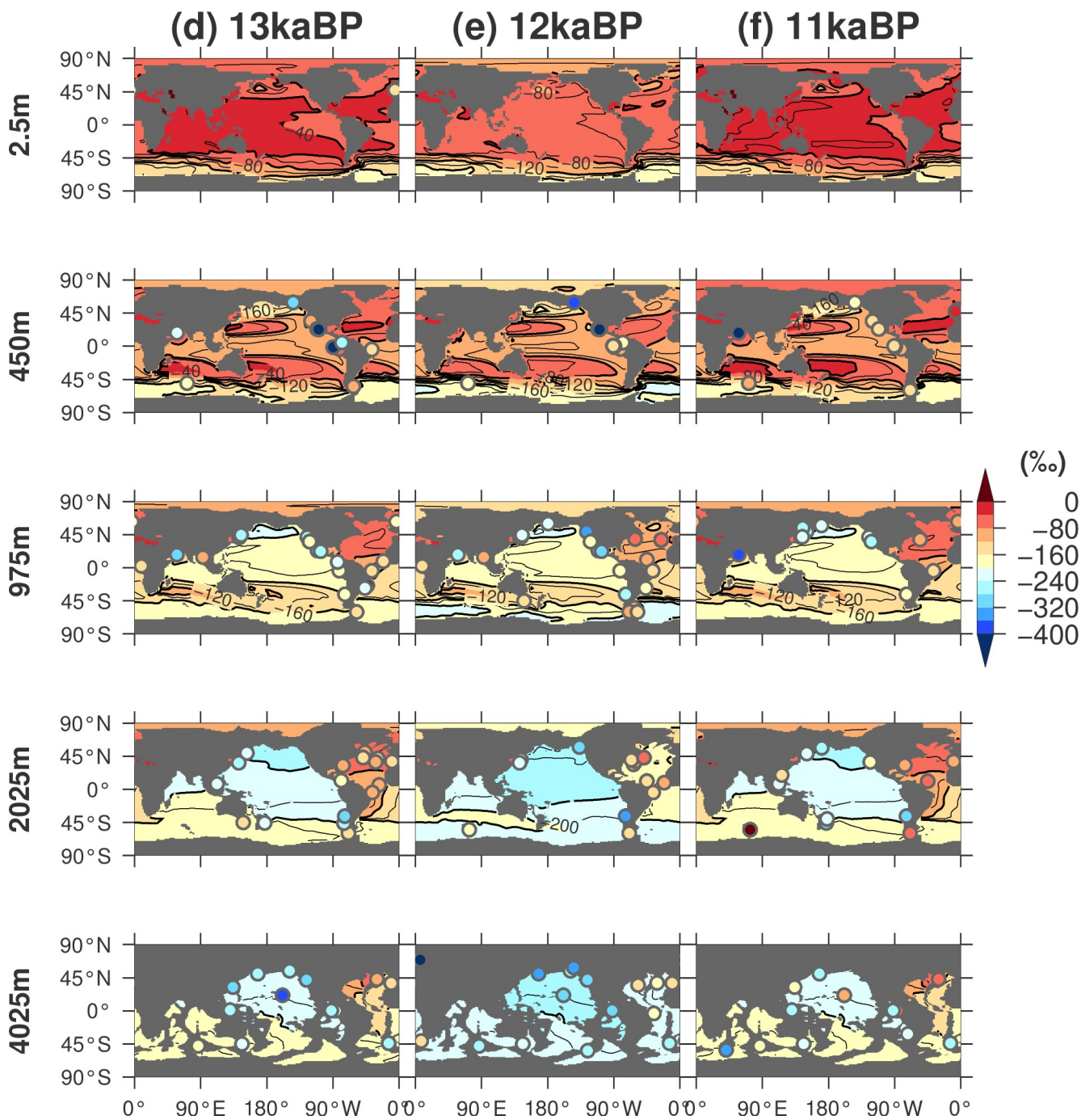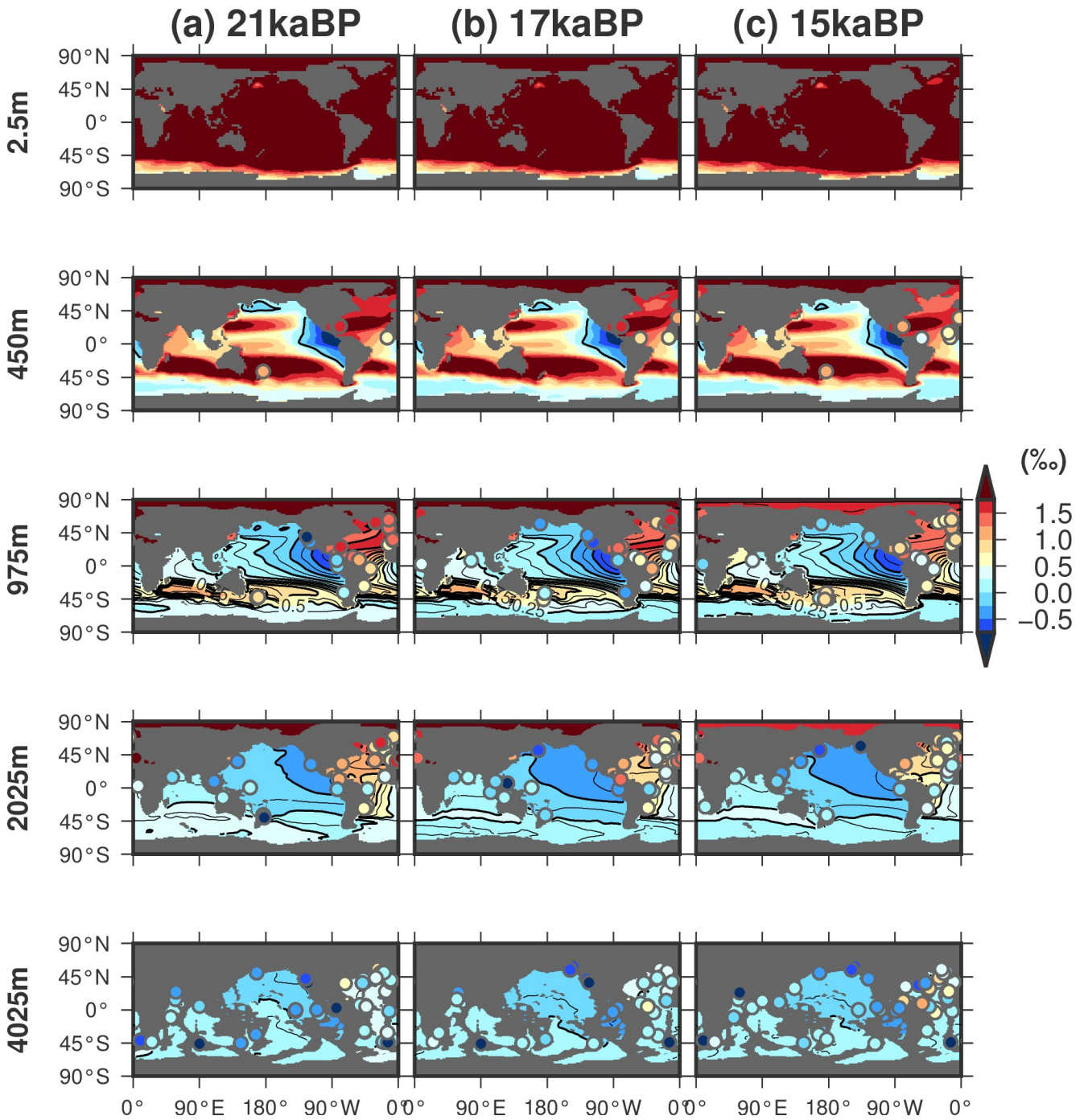
Figure S5: Oceanic distribution of δ^{13}C (‰) at specific depths (2.5 m, 450 m, 975 m, 2025 m, and 4025 m) during the last deglaciation. The contour interval is 0.25 ‰. The sediment core records used in the figure are compiled in *Muglia et al.*, (2023). The period over which the model output is averaged is 100 years before and after each year of interest. The reconstructed values are also plotted for 100 years before and after each year of interest.

Figure S5: (continued)
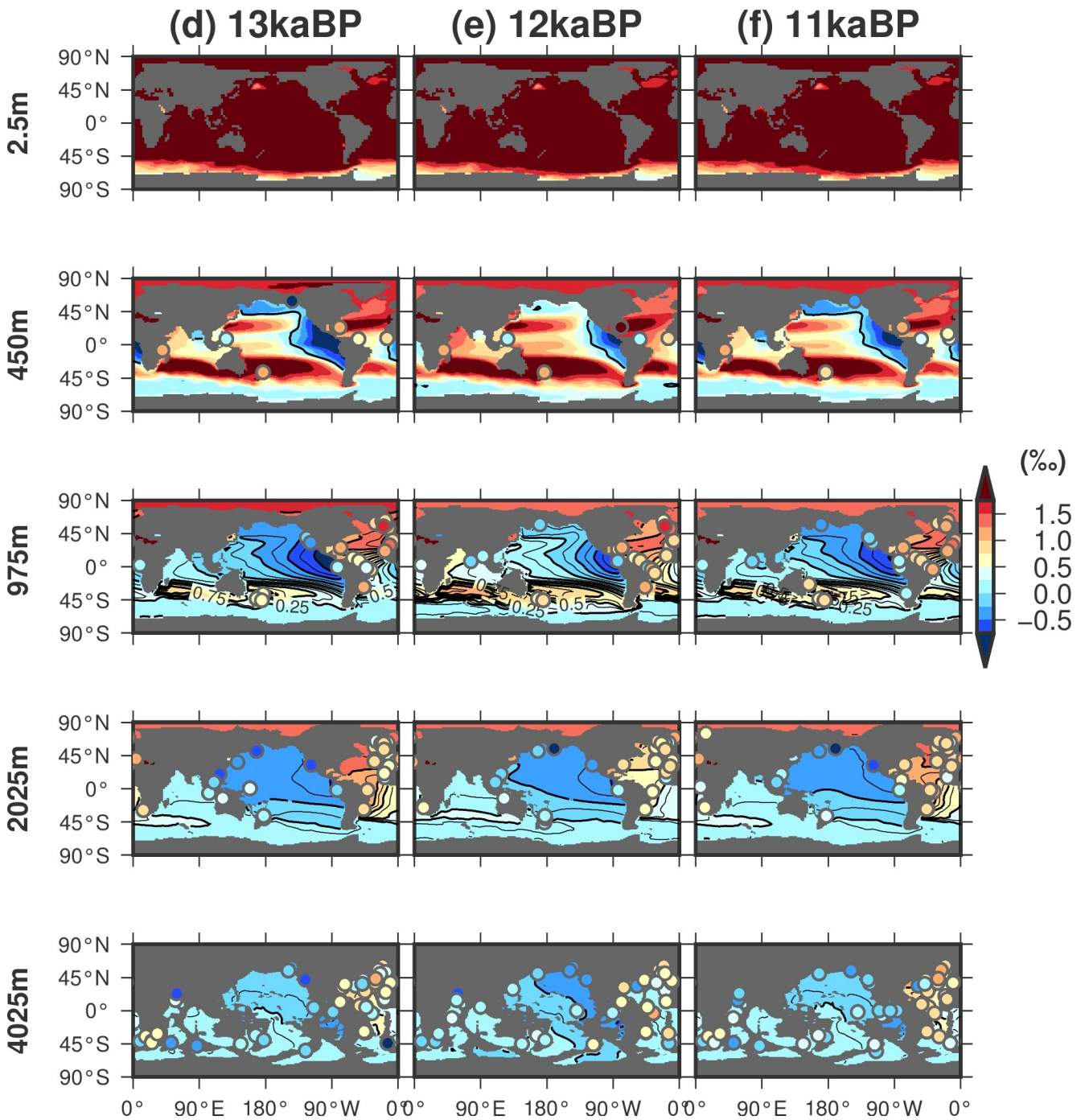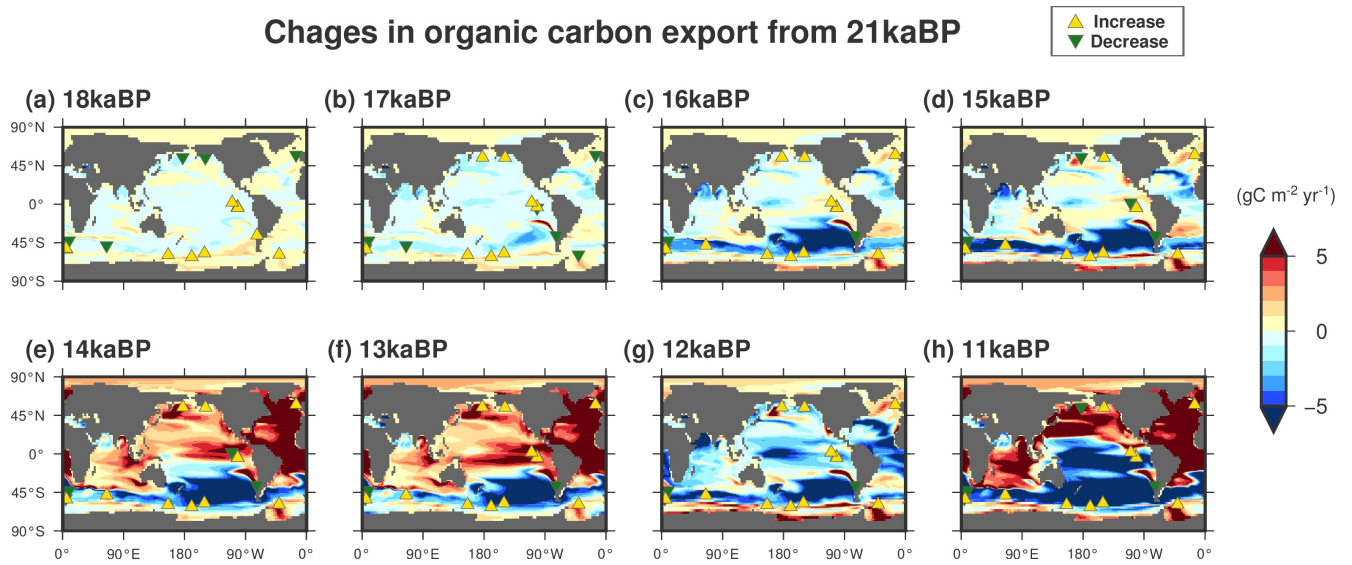
Figure S6: The calculated changes in organic carbon export ($\text{PgC}\,\text{m}^{-2}\,\text{yr}^{-1}$) relative to the values at 21 ka BP are shown. The contour interval is $1\,\text{PgC}\,\text{m}^{-2}\,\text{yr}^{-1}$. The triangles indicate qualitative increases (yellow) or decreases (green) in biological flux. These fluxes are reconstructed from proxies such as opal flux and alkenone flux in sediment core records (*Chase et al.*, 2003; *Anderson et al.*, 2009; *Bolton et al.*, 2011; *Kohfeld and Chase*, 2011; *Martinez-Garcia et al.*, 2014; *Maier et al.*, 2015; *Studer et al.*, 2015; *Thiagarajan et al.*, 2019; *Ai et al.*, 2020; *Weber et al.*, 2021; *Li et al.*, 2022).

Dissolved inorganic carbon
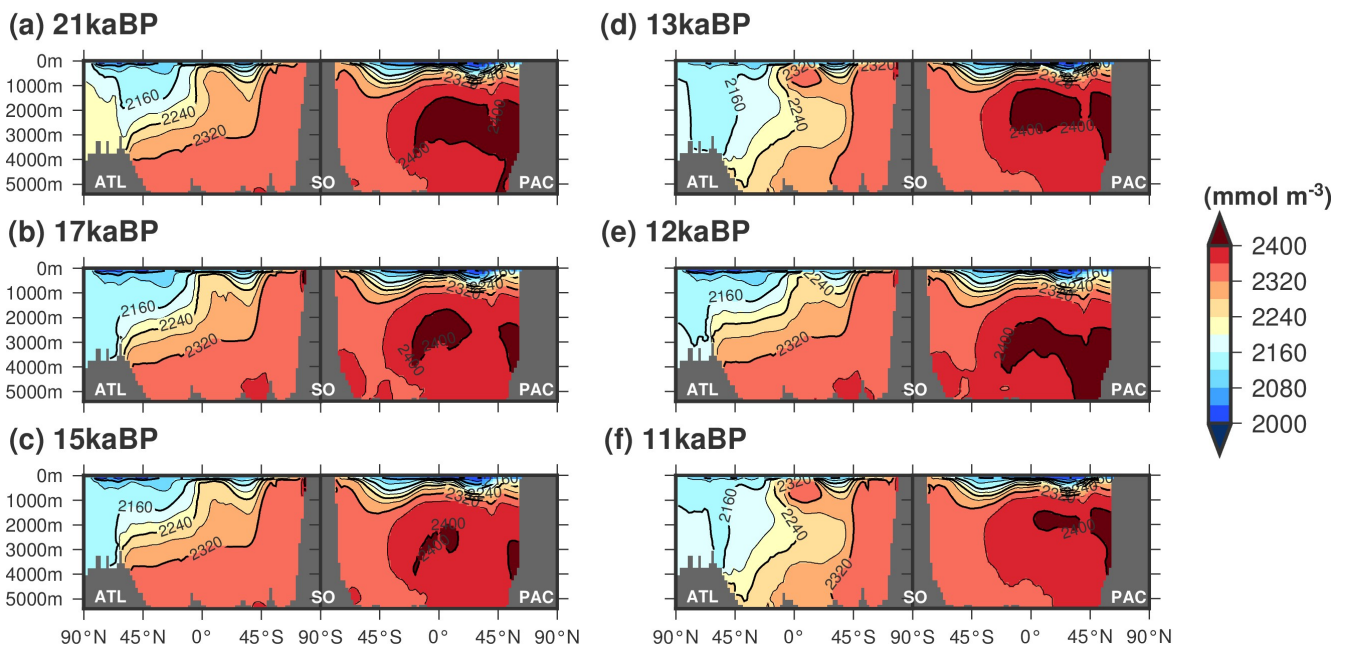
Figure S7: Oceanic zonal mean distribution of dissolved inorganic carbon (mmol m^{-3}) during key periods of the last deglaciation in the Atlantic and Pacific oceans. The specific periods of interest include (a) the Last Glacial Maximum (21 ka BP), (b) Heinrich Stadial 1 (17 ka BP), (c) just before the Bølling-Allerød (BA) transition (15 ka BP), (d) the BA warm period (13 ka BP), (e) the Younger Dryas period (12 ka BP), and (f) the Holocene (11 ka BP). The contour interval is 40 mmol m^{-3}. Model results are averaged over 200 years, i.e., 100 years before and after each target year. However, for 21 ka BP, the average is taken from results spanning 21.0–20.9 ka BP; for 11 ka BP, the average is taken from results spanning 11.1–11.0 ka BP.
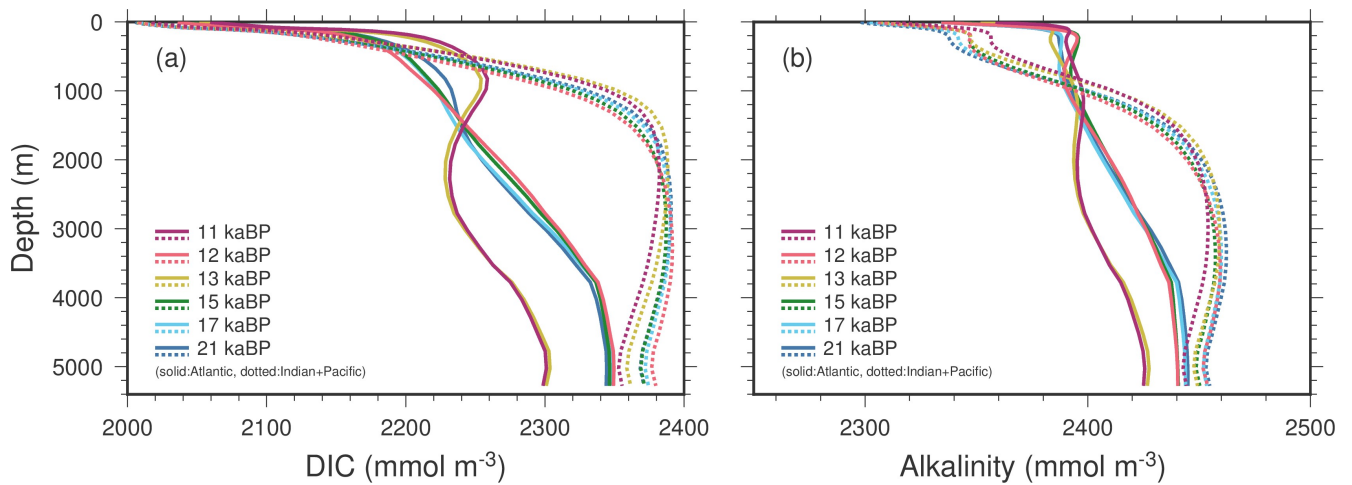
Figure S8: Oceanic vertical one-dimensional distribution of (a) dissolved inorganic carbon (DIC) and (b) alkalinity (mmol m^{-3}) during key periods of the last deglaciation in the Atlantic (solid line) and Pacific oceans (dotted line). The specific periods of interest include the Last Glacial Maximum (21 ka BP), Heinrich Stadial 1 (17 ka BP), just before the Bølling-Allerød (BA) transition (15 ka BP), the BA warm period (13 ka BP), the Younger Dryas period (12 ka BP), and the Holocene (11 ka BP). Model results are averaged over 200 years, i.e., 100 years before and after each target year. However, for 21 ka BP, the average is taken from results spanning 21.0–20.9 ka BP; for 11 ka BP, the average is taken from results spanning 11.1–11.0 ka BP.

References for supplementary information

[] X. E. Ai, A. S. Studer, D. M. Sigman, A. Martínez-García, F. Fripiat, L. M. Thöle, E. Michel, J. Gottschalk, L. Arnold, S. Moretti, M. Schmitt, S. Oleynik, S. L. Jaccard, and G. H. Haug, Southern Ocean upwelling, Earth's obliquity, and glacial-interglacial atmospheric CO_2 change, *Science*, **370**, 1348–1352, https://doi.org/10.1126/science.abd2115, 2020.

[] R. F. Anderson, S. Ali, L. I. Bradtmiller, S. H. H. Nielsen, M. Q. Fleisher, B. E. Anderson, and L. H. Burckle, Wind-Driven Upwelling in the Southern Ocean and the Deglacial Rise in Atmospheric CO_2, *Science*, **323**, 1443–1448, https://doi.org/10.1126/science.1167441, 2009.

[] C. T. Bolton, K. T. Lawrence, S. J. Gibbs, P. A. Wilson, and T. D. Herbert, Biotic and geochemical evidence for a global latitudinal shift in ocean biogeochemistry and export productivity during the late Pliocene, *Earth and Planetary Science Letters*, **308**, 200–210, https://doi.org/10.1016/j.epsl.2011.05.046, 2011.

[] Z. Chase, R. F. Anderson, M. Q. Fleisher, and P. W. Kubik, Accumulation of biogenic and lithogenic material in the Pacific sector of the Southern Ocean during the past 40, 000 years, *Deep Sea Research Part II: Topical Studies in Oceanography*, **50**, 799–832, https://doi.org/10.1016/s0967-0645(02)00595-7, 2003.

[] K. E. Kohfeld and Z. Chase, Controls on deglacial changes in biogenic fluxes in the North Pacific Ocean, *Quaternary Science Reviews*, **30**, 3350–3363, https://doi.org/10.1016/j.quascirev.2011.08.007, 2011.

[] C. Li, V. J. Clementi, S. C. Bova, Y. Rosenthal, L. B. Childress, J. D. Wright, and Z. Jian, The Sediment Green-Blue Color Ratio as a Proxy for Biogenic Silica Productivity Along the Chilean Margin, *Geochemistry, Geophysics, Geosystems*, **23**, https://doi.org/10.1029/2022gc010350, 2022.

[] A. Martínez-García, D. M. Sigman, H. Ren, R. F. Anderson, M. Straub, D. A. Hodell, S. L. Jaccard, T. I. Eglinton, and G. H. Haug, Iron Fertilization of the Subantarctic Ocean During the Last Ice Age, *Science*, **343**, 1347–1350, https://doi.org/10.1126/science.1246848, 2014.

[] E. Maier, M. Méheust, A. Abelmann, R. Gersonde, B. Chapligin, J. Ren, R. Stein, H. Meyer, and R. Tiedemann, Deglacial subarctic Pacific surface water hydrography and nutrient dynamics and links to North Atlantic climate variability and atmospheric CO_2, *Paleoceanography*, **30**, 949–968, https://doi.org/10.1002/2014pa002763, 2015.

[] J. Muglia, S. Mulitza, J. Repschläger, A. Schmittner, L. Lembke-Jene, L. Lisiecki, A. Mix, R. Saraswat, E. Sikes, C. Waelbroeck, J. Gottschalk, J. Lippold, D. Lund, G. Martinez-Mendez, E. Michel, F. Muschitiello, S. Naik, Y. Okazaki, L. Stott, A. Voelker, and N. Zhao, A global synthesis of high-resolution stable isotope data from benthic foraminifera of the last deglaciation, *Scientific Data*, **10**, https://doi.org/10.1038/s41597-023-02024-2, 2023.

[] P. A. Rafter, W. R. Gray, S. K.V. Hines, A. Burke, K. M. Costa, J. Gottschalk, M. P. Hain, J. W.B. Rae, J. R. Southon, M. H. Walczak, J. Yu, J. F. Adkins, and T. DeVries, Global reorganization of deep-sea circulation and carbon storage after the last ice age, *Science Advances*, **8**, https://doi.org/10.1126/sciadv.abq5434, 2022.

[] A. S. Studer, D. M. Sigman, A. Martínez-García, V. Benz, G. Winckler, G. Kuhn, O. Esper, F. Lamy, S. L. Jaccard, L. Wacker, S. Oleynik, R. Gersonde, and G. H. Haug, Antarctic Zone nutrient conditions during the last two glacial cycles, *Paleoceanography*, **30**, 845–862, https://doi.org/10.1002/2014pa002745, 2015.

[] N. Thiagarajan and J. F. McManus, Productivity and sediment focusing in the Eastern Equatorial Pacific during the last 30, 000 years, *Deep Sea Research Part I: Oceanographic Research Papers*, **147**, 100–110, https://doi.org/10.1016/j.dsr.2019.03.007, 2019.

[] M. E. Weber, Antiphased dust deposition and productivity in the Antarctic Zone over 1.5 million years, https://doi.org/10.1594/PANGAEA.939650 2021.